

1 Ice and air: Visualisation of freeze-thaw embolism and freezing spread in 2 young *L. tulipifera* leaves

3 Kate M. Johnson¹, Muriel Scherer², Dominic Gerber², Robert W. Style², Eric R. Dufresne^{2,3}, Craig R.
4 Brodersen¹

5 ¹ Centre de Recerca Ecològica i Aplicacions Forestals (CREAF), Barcelona, Spain

6 ² Eidgenössische Technische Hochschule (ETH), Department of Materials, Zürich, Switzerland

7 ³ Cornell University, Materials Science and Engineering, New York, USA

8 ⁴ Yale University School of the Environment, New Haven, Connecticut, USA

9

10 **Authors for correspondence:** Kate M. Johnson, email: kate.johnson@utas.edu.au , Craig R.
11 Brodersen, email: craig.brodersen@yale.edu

12 **ORcIDs:** Kate M. Johnson: <https://orcid.org/0000-0002-3039-6339>, Muriel Scherer:
13 <https://orcid.org/0000-0003-3777-8206>, Dominic Gerber: <https://orcid.org/0000-0002-4231-0694> ,
14 Robert W. Style: <https://orcid.org/0000-0001-5305-7658>, Eric R Dufresne: <https://orcid.org/0000-0002-3091-5039>, Craig R. Brodersen: <https://orcid.org/0000-0002-7154-2822>

16 Summary

- 17 - Spring freezing is an unforgiving stress for young leaves, often leading to death, with
18 consequences for tree productivity and survival. While both the plant water transport
19 system and living tissues are vulnerable to freezing, we do not know whether
20 damage to one or both of these systems causes death in young leaves exposed to
21 unseasonal freezing.
- 22 - Whole saplings of *Liriodendron tulipifera* were exposed to freezing and thawing
23 trajectories designed to mimic spring freezes in nature. We visualised freezing
24 damage to the water transport system (xylem embolism) and living tissues
25 (mesophyll freezing, decline in chlorophyll fluorescence).
- 26 - We 1.) provide the first visualisation of freeze-thaw embolism in leaves, 2.) reveal a
27 predictable progression of ice formation within the mesophyll which is strongly
28 influenced by leaf vein architecture, notably the presence or absence of bundle
29 sheath extensions, and 3.) show that freeze-thaw embolism occurs only in the largest
30 vein orders where mean vessel diameter exceeds 30µm.
- 31 - With evidence of both freeze-thaw embolism and damage to photosynthetic tissue,
32 we conclude that this dual-mode lethality may be common among other wide-
33 vesseled angiosperm-leaves, potentially playing a role in limiting distributions, and
34 show that bundle sheath extensions may stall or even prevent freezing spread.

35 **Key words:** Embolism, Fluorescence, Freezing, Freeze-thaw embolism, Leaves, Optical
36 imaging, Spring-freezing.

37 **Introduction**

38 Freezing is one of the strongest determinants of plant distributions (Burke, Gusta et al. 1976,
39 Loehle 1998, Sakai and Larcher 2012, Muffler, Beierkuhnlein et al. 2016), owing to the
40 unforgiving and often lethal nature of freezing in plant tissues that are not specifically
41 equipped to avoid, resist or compartmentalise ice crystal formation (Burke, Gusta et al. 1976,
42 Stegner, Buchner et al. 2023). Some trees have adaptations to prevent or tolerate freezing
43 within their tissues year-round, while others, such as those in temperate regions, are
44 adapted only to seasonal winter-freezing (Burke, Gusta et al. 1976, Wisniewski and Fuller
45 1999, Sakai and Larcher 2012). Both the xylem and living leaf tissue are critical to consider
46 when assessing the effects of freezing, as damage to plant water transport or the sites of
47 photosynthesis jeopardise tree growth and survival (Brodribb, Brodersen et al. 2021).

48 Within branches and tree-trunks, xylem anatomy is known to influence the likelihood of
49 freezing damage. During freezing, gas bubbles become suspended in the xylem sap as the
50 crystallization process pushes dissolved gasses out of solution. Upon thawing, these
51 bubbles either dissolve back into solution or expand to fill xylem conduits and block water
52 flow depending on the pressure of the surrounding liquid (Hammel 1967, Sperry and Sullivan
53 1992, Hacke and Sauter 1996). Species with larger diameter xylem conduits have been
54 shown to be more vulnerable to 'freeze-thaw embolism' (Sperry and Sullivan 1992, Feild and
55 Brodribb 2001, Tyree and Zimmermann 2002, Cavender-Bares, Cortes et al. 2005, Sevanto,
56 Holbrook et al. 2012, Li, Luo et al. 2024), with mean conduit diameter shown to decrease
57 with increasing likelihood of freezing conditions (Sperry 1995). There are a number of
58 possible explanations for this. Larger vessels have been shown to embolise earlier than
59 smaller vessels exposed to freezing (Davis, Sperry et al. 1999, Cavender-Bares, Cortes et
60 al. 2005). Additionally, smaller conduits have been shown, in some cases, to freeze at higher
61 velocity which lead to smaller air bubbles (Ewers 1985) which are more easily dissolved
62 upon thawing (Sevanto, Holbrook et al. 2012).

63 Winter deciduousness allows many angiosperm trees (and some gymnosperms) to avoid
64 leaf-level freezing damage, but does not protect spring growth, nor leaves that persist into
65 autumn. In particular, freezes after bud-burst in spring can have severe consequences for
66 deciduous trees (Burke, Gusta et al. 1976, Vitasse, Bottero et al. 2019). While winter-
67 deciduousness allows deciduous trees to avoid winter frost-damage to leaves, spring frosts
68 often kill or damage leaves (Burke, Gusta et al. 1976), which has been shown to cause a
69 strong reduction in tree growth (Vitasse, Bottero et al. 2019).

70 Leaf senescence is not the only strategy that deciduous trees employ to protect their tissues
71 against freezing damage: dormancy and other 'hardening' processes have evolved to

72 prevent or limit the formation of ice in the living tissue of these trees, which can occur inside
73 cells (intracellular) or outside cells (intercellular). Intracellular ice formation invariably leads
74 to cell death by rupture of the cell membranes, caused by internal nucleation of piercing by
75 external ice crystals (Mazur 1969, Burke, Gusta et al. 1976, Steponkus, Dowgert et al. 1983,
76 Guy 1990). Extracellular ice formation can also result in cell death by creating a water
77 potential gradient which draws out cellular water to feed the freezing-front (Guy 1990,
78 Steponkus and Webb 1992), therefore imposing a desiccation stress resembling that caused
79 by drought (Ruelland, Vaultier et al. 2009, Vitra, Lenz et al. 2017, Yang, Gerber et al. 2024).
80 To combat ice formation within or between cells, beyond autumn, meristematic tissues in the
81 buds of winter-deciduous trees enter dormancy when environmental conditions are
82 unsuitable for growth (Lang 1987, Sapkota, Salem et al. 2023). During this period, cell
83 activity within leaf and flower buds slows, with this delicate tissue encapsulated by protective
84 bud-scales (Nilsson 2022).

85 Spring frost may be lethal in young leaves through at least two different modes that are not
86 mutually exclusive. First, ice formation in or around the living tissues poses a significant
87 threat because of the potential damage to cell walls and membranes leading to electrolyte
88 leakage, damage to organelles and the generation of reactive oxygen species (Wise 1995,
89 Lütz 2010). Second, embolism formation resulting from the freezing and thawing of the
90 xylem sap could lead to complete failure of the leaf vein network thereby cutting off the
91 supply of water to downstream tissues (Brodribb et al. 2021). While the effects of freeze-
92 thaw embolism have been well documented in stems (Sperry, Donnelly et al. 1988, Feild and
93 Brodribb 2001, Ashworth and Pearce 2002, Cobb, Choat et al. 2007, Mayr, Schmid et al.
94 2014, Robinson, Rennie et al. 2023), this has never been visualised in leaves.

95 The primary means of tracking the propagation of freezing damage through whole leaves
96 has been with high temporal resolution using multiple forms of thermal imaging (Larcher,
97 Meindl et al. 1991, Gusta, Wisniewski et al. 2004, Hacker and Neuner 2007, Kokin, Pennar
98 et al. 2018, Zhang, Han et al. 2023). Hacker and Neuner (2007) in particular provide key,
99 novel information about ice nucleation and freezing relative to leaf anatomy, showing ice
100 nucleation beginning in the veins and spreading through the mesophyll tracking leaf
101 venation, however this is one of few papers to consider the influence of leaf venation on ice-
102 spread. While thermal imaging with very high temporal resolution (Hacker and Neuner 2007;
103 25 images per second) and some optical imaging (Kokin, Pennar et al. 2018) have been
104 used to study leaf freezing; longer-term high resolution imaging of leaves during freezing and
105 thawing has not been conducted. Given that ice crystallization is often lethal in living tissues
106 and that leaf cells are also supplied by a vascular system that is vulnerable to freeze-thaw
107 embolism, one of the goals of the present study was to provide a detailed characterisation of

108 ice formation in leaf tissue by visualising freezing and thawing in the leaves of intact plants, a
109 process has recently been undertaken in a freeze resistant species (Kane and McAdam
110 2024) but never in young, likely freeze-intolerant leaves. Using this information, we could
111 assess the probable cause of leaf death (embolism, cell damage or a combination of both)
112 due to spring frost.

113 Here we visualise the effects of freezing and thawing on both the living cells and the xylem in
114 young leaves in *Liriodendron tulipifera*, a common deciduous tree in North America. To
115 detect possible embolism and track ice crystal formation in leaves we used a combination of
116 time-lapse imaging and chlorophyll fluorescence imaging to non-invasively study young
117 leaves of *L. tulipifera* saplings exposed to freezing conditions, with minimum air-
118 temperatures ranging from -1 to -5 °C. By capturing images of newly expanded leaves at
119 regular intervals throughout freezing and thawing we aimed to elucidate the pattern of
120 freezing spread in these leaves and capture any embolism that may occur using the Optical
121 Vulnerability Method of Brodribb et al. (2017). We then measured chlorophyll fluorescence of
122 leaf tissue before and after freezing as a proxy for tissue damage (Brodribb et al. 2021). To
123 compare the effect of freeze-thaw embolism vs. drought-induced embolism, thereby partially
124 isolating the effect of freezing on the living cells in the leaf, we tracked drought-induced
125 embolism in leaves of the same age.

126 *L. tulipifera* has been shown to possess bundle sheath extensions (BSEs), structures that
127 connect the bundle sheath and the epidermis and influence a range of physiological process
128 in plants relating to both photosynthesis and hydraulics (Wylie 1943, Wylie 1952, Pray 1954,
129 Esau 1960 ; Fig S1, Zwieniecki, Brodribb et al. 2007). Bundle sheath extensions
130 compartmentalise the leaf lamina restricting the movement of gases therefore allowing gas
131 exchange to occur independently across the leaf surface, with the leaves, and species
132 possessing these, been termed heterobaric (Neger 1918). Assimilation has been shown to
133 be higher in species with BSEs (Karabourniotis, Bornman et al. 2000), with these structures
134 also shown to influence leaf hydraulics and drought tolerance (Kawai, Miyoshi et al. 2017).
135 In leaves, upon exiting the xylem, water is transferred to the bundle-sheath (Trifiló,
136 Raimondo et al. 2016). By connecting the veins and the epidermis, BSEs have been shown
137 to assist in supplying water from veins to stomata (Zwieniecki, Brodribb et al. 2007) and also
138 reduce the resistance to water flow between the bundle sheath and the epidermis (Buckley,
139 Sack et al. 2011). Highly sclerified BSEs have also been shown to prevent the lateral
140 prorogation of ice in the lamina in *Cinnamomum canphora*, yet this is the only species in
141 which this has been documented (Hacker and Neuner 2007, Barbosa, Chitwood et al. 2019).
142 In *L. tulipifera* BSEs extend to both the upper and lower epidermises in second order and
143 third order veins (Pray 1954; Fig S1), while they extend only to the abaxial epidermis in

144 higher order veins (Pray 1954).(Pieruschka, Schurr et al. 2006, Barbosa, Chitwood et al.
145 2019). It is possible that even the non-sclerified bundle-sheath extensions in *L. tulipifera*
146 could act as a barrier to the ice crystallization front as it progresses across the lamina, which
147 led us to attempt to determine their influence in this species.

148 Based on the known physical processes that govern ice nucleation and growth in laminar
149 systems that superficially resemble leaves, we expected ice to first form in leaf regions with
150 low solute content, and therefore a higher freezing temperature, such as the midveins
151 containing numerous xylem conduits loaded with xylem sap. Ice would then propagate
152 outward across the lamina as temperature decreases below the freezing point of the
153 surrounding tissues with higher solute content. Given that the BSEs represent a physical
154 barrier that would slow the movement of water toward the ice nucleation front, we expected
155 BSEs to significantly influence the spatial pattern and progression of ice across the lamina,
156 which would be most noticeable in the higher order veins where BSEs span both the upper
157 and lower epidermis. We developed two possible working hypotheses for freeze-thaw
158 embolism: 1.) Freeze-thaw embolism would occur upon thawing in a pattern resembling
159 embolism caused by drought, where the lower vein orders embolize first, followed by the
160 higher order veins; or 2.) Embolism would occur only in veins with large vessel diameters
161 (equal to or > 30 μm) based on research in stems which shows a steep increase in freeze
162 thaw embolism in conduits above this threshold (Pittermann and Sperry 2006). Finding this
163 would suggest that conduit size may govern the occurrence of freeze-thaw embolism across
164 organs. We predicted that ice crystal formation would lead to damaged cell walls and
165 membranes and thus irreparable damage to the mesophyll, made visible by significant
166 decreases in chlorophyll fluorescence shortly after thawing. If freeze-thaw embolism
167 occurred, it would lead to cell death in any remaining un-frozen tissue but over a longer time
168 period. The combined effects of these processes may explain the universality of leaf death
169 due to spring frost across broad-leaved tree species.

170 **Materials and Methods**

171 *Freezing experiment*

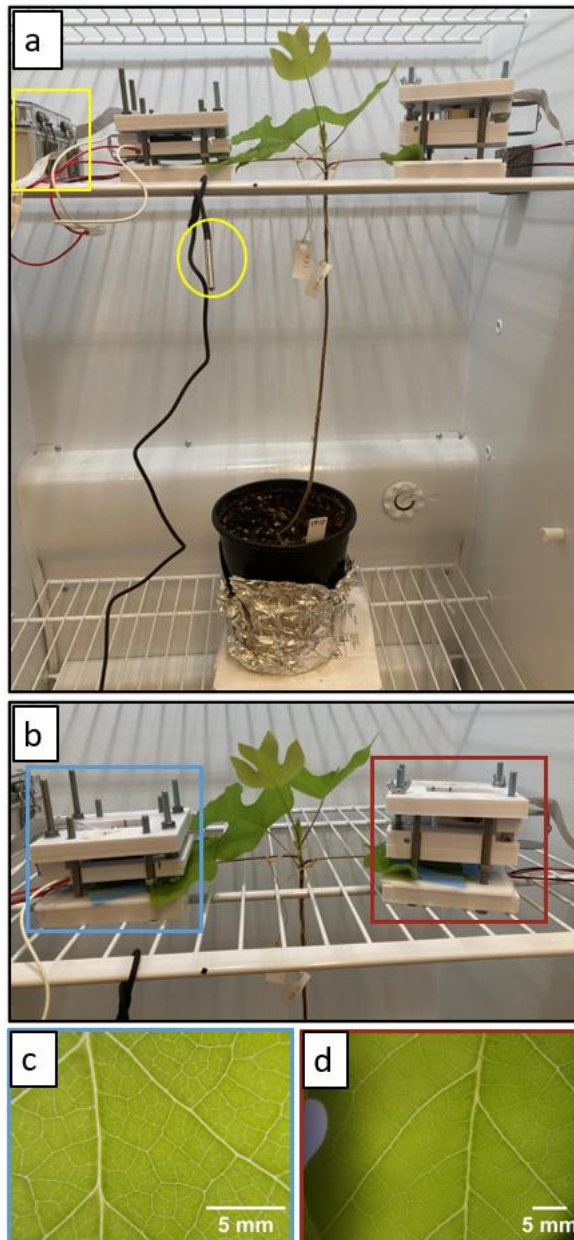
172 Saplings of *Liriodendron tulipifera* (~ 2 years old) were grown under glasshouse conditions
173 (day temperature of ~25-30 C and night temperatures of ~ 15-20 C) for 1.5 months, until
174 there were at least two fully expanded leaves per tree, before experimentation (conducted
175 between March and May 2022). A total of 13 trees were frozen to one of five minimum
176 freezing temperatures (-1, -2, -3, -4 or -5 °C). We selected this range of minimum
177 temperatures to both determine the temperature needed to fully freeze leaves, but also to

178 test the effects of cold temperatures that did not induce freezing. We used the Optical
179 Vulnerability Method (OVT) of Brodribb et al. 2017 to monitor both the formation of embolism
180 but also the changes in optical density of the mesophyll associated with freezing. We imaged
181 a total of 24 leaves and one main stem. Each tree was frozen as described below.

182 Saplings growing in pots were placed in an upright freezer (Model: FFFH20F2QWC,
183 Electrolux home products Inc.) which was attached to a thermostat (Model: ITC-310T-B,
184 Inkbird dual relay) which was used to control the freezing trajectory. Two adjacent fully
185 expanded leaves were placed inside 'cavacam' imaging clamps (docs.cavcams.com, Fig. 1).
186 Briefly, a digital raspberry pi camera (V2, 9132664) was positioned to observe the adaxial
187 leaf surface and transmitted light is provided by a digitally controlled set of LED lights that
188 only illuminate during image capture (Brodribb, Bienaime et al. 2016). Cameras were set to
189 capture images every 5 minutes during freezing and thawing, a process that was
190 programmed to occur over 20 hours (see details below). A custom-built temperature logger
191 'envirologger' run by a data-logger (Adafruit feather M0 Adalogger) was placed in the freezer
192 to track the internal conditions with a temperature/humidity sensor (Model: AM2315 12C,
193 Adafruit).

194 The freezing sequence and trajectory were based on winter/spring temperature data from a
195 weather station (Campbell Scientific CR300) monitoring windspeed, air temperature, relative
196 humidity, precipitation, soil moisture and soil temperature, averaged hourly over the
197 measurement period) at nearby Yale Myers Forest (Union, CT, USA; 41° 57' 8.2944" N, 72°
198 7' 26.688" W), where *L. tulipifera* trees are known to grow, in order to mimic the freezing
199 conditions experienced by this species under natural conditions. A representative night in
200 2019 where temperatures reached -5 °C was chosen as a reference. The temperature data
201 from Yale Myers Forest (recorded half-hourly) was averaged and rounded to the nearest
202 whole number to determine mean hourly temperatures. These temperatures were then
203 used to inform a 12-step programmed freezing sequence. This resulted in a stepped freezing
204 sequence that ran for approximately 20 hours (including an ~ 6 hour period at a positive
205 temperature at the end) mimicking an overnight freezing event (Fig S2).

206
207
208
209
210
211
212
213
214
215
216
217
218
219
220
221
222
223
224
225



226 **Figure 1:** The set-up for monitoring freeze in *L. tulipifera* trees. Panel (a) shows the sapling inside the
227 freezer with cameras attached. The unit for measuring freezer air temperature is denoted by a yellow
228 box while the temperature probe attached to the device controlling the freeze trajectory is circled in
229 yellow. In panel (b) the two cameras are distinguished by boxes, with the higher magnification
230 camera in blue and lower magnification camera in red. Corresponding images taken by each camera
231 are shown below the respective cameras, in boxes of the same colours (blue; higher magnification
232 and red; lower magnification) with a 5mm scale bar in the bottom right-hand of each image.

233 *Chlorophyll Fluorescence Imaging*

234 To determine the physiological effects of freezing temperatures on leaves we used
235 chlorophyll fluorescence imaging, which provides a measure of the status of the
236 photosynthetic apparatus and its capacity for processing light. We performed dark-adapted

237 Fv/Fm imaging on leaves both before freezing to provide a baseline reference measurement,
238 and then again after freezing to determine how much the photosystems were damaged (Mini
239 Imaging-PAM M-series, Walz GmbH, Germany). Before fluorescence measurements, a
240 small piece of opaque tape was applied to a small section (~ 0.5x 0.5 cm) of the leaf, then
241 the leaves were wrapped in aluminium foil to exclude light. The patch of opaque tape was
242 used because initial testing showed that, as removal of aluminium foil was required to align
243 the leaf under the imaging PAM, an initial measure was needed to maintain some leaf tissue
244 in the dark-adapted state required for Fv/Fm measurements. The tape was removed
245 seconds before measurement to ensure that the leaf tissue beneath the tape remained fully
246 dark adapted until fluorescence was measured.

247 *Freezing and thawing in the leaf mesophyll*

248 Image sequences were processed in FIJI software (Schindelin, Arganda-Carreras et al.
249 2012) to determine the spread and extent of ice crystallization during the experiments. The
250 tracing tool in FIJI was used to quantify the total leaf area frozen at each time step, which
251 was indicated by a change in the colour intensity of the pixels. Freezing was detected as
252 patches of brighter pixels in the leaf lamina, typically bounded by higher order veins.

253 To quantify the colour change in both mesophyll tissue that did and did not freeze, circular
254 ROIs of 40x40 pixels were selected in regions of both mesophyll that froze and that which
255 did not in all leaves frozen to -4 °C. The mean grey scale value in these ROIS was
256 calculated at three time-points, at the start of image capture, at -4 °C and immediately after
257 thawing. The values at -4 °C and after thawing were expressed as a percentage of the initial
258 mean greyscale value (from the start of image capture) and the average percentage of the
259 initial value was calculated for both frozen and unfrozen mesophyll.

260 A similar method, utilising circular ROIs in FIJI, was used to track the change in mean
261 greyscale area in the midveins and mesophyll of all leaves which experienced freezing. In
262 each leaf, ROIs which fit within the diameter of the midvein were selected and added to the
263 ROI manager. This was repeated across the image stack or up to 250 images (where more
264 images were recorded), with the ROI shifted using 'edit>selection>specify' when the leaf
265 moved. The 'Interpolate ROI's' option through the ROI manager was then used to interpolate
266 between the selected ROIs for all images. The 'measure' function was then used to calculate
267 the mean greyscale area in the selected ROI for each image. This was then repeated for a
268 section of mesophyll adjacent to the midvein, using an ROI of the same area. The mean
269 greyscale values across the images were expressed as a percentage of the initial (unfrozen)
270 mean greyscale value in order to generate lines plots of changes in mean grey scale value
271 before, during and after freezing.

272 The freezing extent was calculated in the image where the maximum amount of tissue was
273 frozen, which corresponded with the minimum air temperature to which the leaves were
274 exposed. The frozen regions were selected using the tracing tool in FIJI (Schindelin,
275 Arganda-Carreras et al. 2012) and expressed as percentage of the total visible leaf area
276 within the field of view to calculate a percentage.

277 *Embolism upon thawing*

278 We monitored the leaf vein network for the formation of embolism using the OVT (Brodrigg,
279 Bienaime et al. 2016). Freeze-thaw embolism was analysed using the same methodology
280 which is used to highlight drought-induced embolism with leaf images analysed via an image
281 subtraction, where each image is subtracted from the one before to reveal the changes
282 between the images. As there is a change in light transmission as air rapidly replaces water
283 in the xylem due to embolism, the image subtraction reveals these changes which can then
284 be visualised through time. A detailed description of the methodology used to process
285 images can be found here: <https://www.opensourceov.org/>. While embolism was expected
286 to occur upon thawing, cameras remained attached to plant organs for ~6 hours to ensure
287 that all embolism was captured.

288 *Drought embolism*

289 Optical analysis of embolism was undertaken in a total of six leaves from branches of adult
290 trees, one leaf was sourced from a tree located on the Yale University campus, New Haven,
291 Connecticut, USA (41°19'16.6"N 72°55'25.8"W), and the remaining five leaves were
292 sampled from across four trees located in North Hobart, Tasmania, Australia (42°52'07.6"S
293 147°18'57.8"E). Young, fully expanded leaves (as a similar developmental stage as those
294 used in the freezing experiment) were chosen for imaging. One leaf from each branch was
295 placed within an imaging clamp and set to take images at 5-minute intervals as the branches
296 dried. Embolism was determined to have finished after 12 hours without embolism. Images
297 were analysed using an image subtraction, as described above.

298 *Analysis of embolism*

299 The timing and extent of embolism were determined both in leaves exposed to freezing and
300 those exposed to drought. To visualise embolism through time, embolism was colour coded
301 according to time in both a leaf exposed to freeze and a leaf exposed to drought. This was
302 done using FIJI (Schindelin, Arganda-Carreras et al. 2012) using the 'colour slices' function
303 in the 'OSOV toolbox', the toolbox and instructions are available here:
304 <https://www.opensourceov.org/>.

305 *Embolism and vein order*

306 To determine how much the vein network embolised, the total length of the visible venation
307 network was calculated along with the total area of the embolised vein network using the
308 'segmented line' tool in image J and the embolised vein area was then expressed as a
309 percentage of the vein network. Total vein area was calculated from a raw image of each
310 leaf taken from the stack of images which captured during the drought or freezing treatment
311 while total embolised vein area was calculated from the 'Z- stack' showing all the embolism
312 which occurred during the treatment. Total embolised vein area was then expressed as a
313 percentage of total vein area visible with the optical cameras. As embolism was only
314 observed in the mid-rib and major veins in response to freeze, only these vein orders were
315 included in calculations of vein length and embolised vein length for frozen leaves. The raw
316 images of the vein network and Z-stacks of embolism from leaves exposed to drought were
317 segmented into four even quadrants using a macro in FIJI and the top right corner was
318 analysed for each leaf in order to provide a random sample of the vein network.

319 In *L.tulipifera* leaves, the midvein, second order and tertiary veins are deemed the 'major
320 veins' while the fourth, fifth and sixth and seventh order veins are considered the 'minor'
321 veins and make up the majority of the venation network (Pray 1954).

322 To quantify the contribution of the midvein and second order veins to the earliest embolism
323 in leaves exposed to drought, 25% (embolised area) of the total drought-induced embolism
324 was chosen as a reference value. This was in order to determine whether embolism
325 observed due to freezing and thawing matched early embolism during drought. At this
326 percentage embolism, in all droughted leaves, we calculated both the area contribution of
327 these veins compared to higher vein orders, and the total length of midvein and second
328 order veins embolised as a percentage of the total embolised area of these veins at 100%
329 embolism. For area, the 'freehand sections' tool in FIJI was used to 'circle' all vein orders
330 except for the midvein and second order veins and the area of these veins was calculated
331 using the 'measure' function and expressed as a percentage of the total cumulative
332 embolised area at 25% embolism. The resulting percentage of higher-order-veins was
333 subtracted from 100% to reveal the percentage contribution of the midvein and second order
334 veins to the embolised area at 25 % embolism. For vein length, the 'segmented line' tool was
335 used to calculate the length of the total embolised area of the midvein and second order
336 veins in a Z-stack of the cumulative embolism at 25% embolism. This was expressed as a
337 percentage total embolised midvein and second order vein length at 100% embolism.

338 *High resolution freezing*

339 Branches of adult *L. tulipifera* trees were excised from individuals on the EPFL campus,
340 Lausanne, Switzerland (46.5191° N, 6.5668° E) and transported to the ETH Honggerberg
341 Campus in Zurich. Small leaves were mounted between two glass microscope slides and
342 placed on a customised freezing stage beneath a compound microscope using confocal
343 microscopy (Yokogawa Spinning Disk and Nikon Eclipse, set up & software by 3i imaging).
344 The set-up used is described in (Gerber, Wilen et al. 2023) and the documentation is
345 available at: https://github.com/dogerber/temperature_gradient_microscopy_stage/tree/main.
346 A CF640 filter was used to visualise eaves, capturing the autofluorescence of chlorophyll
347 therefore highlighting the cells in the images.

348 *Xylem conduit diameter analysis*

349 Young *L. tulipifera* leaves were collected from trees and brought to the lab. Vein samples
350 from three leaves were used for the conduit diameter analysis. Midvein samples were
351 collected 1cm from the petiole lamina junction. Second and third order veins were collected
352 0.5 cm from the junction with the subtending lower order vein. Samples were mounted to a
353 freezing stage (BFS-3MP, Physitemp Instruments, USA) on a sliding microtome encased in
354 a dilute glucose solution. Thin sections were stained with a 0.5% toluidine blue solution,
355 rinsed in DI water, and then mounted in water. Images were captured with a digital camera
356 mounted to a compound light microscope (BX43, Olympus Inc, Japan) using a 4x or 10x
357 objective lens. Images were then used to measure xylem vessel diameter in FIJI. Vessel
358 diameter was measured as the longest distance across the lumen.

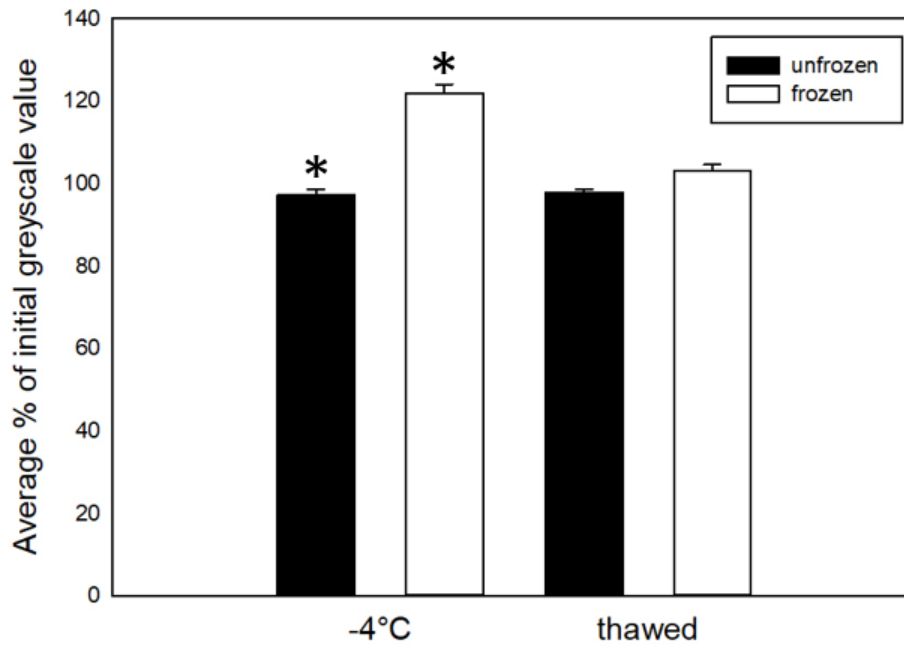
359 *Data analysis*

360 Data were plotted and analysed using SIGMAPLOT v.12.5 (Systat software 2003) and
361 RStudio was used to perform Single factor ANOVAs to determine statistical differences
362 between groups in RStudio (2016). Xylem vessel diameter analysis was performed in
363 RStudio using the dplyr package (Yarberry and Yarberry 2021).

364 **Results**

365 *Pattern of Freezing and thawing*

366 We observed mesophyll freezing in all leaves which were exposed to minimum air
367 temperatures of -4° C or -5° (total of 18 leaves). At -4° C greyscale pixel values increased in
368 the freezing regions that can be interpreted as a change from air to water in the intercellular
369 space as water is drawn out of the mesophyll cells to feed the freezing front (Fig. 2).



381 **Figure 2:** The average percentage of initial (pre-treatment) mean greyscale value (brightness) for all
382 18 leaves that froze, comparing tissue that did and did not freeze within the same leaves. These
383 values were calculated at -4 °C and immediately after thawing. Unfrozen tissue is shown in black,
384 while frozen tissue in shown in white. This was calculated for all 18 leaves that froze. Asterix's
385 indicate a statistically significant difference ($P < 0.05$).

386 While an increase in mean greyscale value, indicating freezing, was always detected in the
387 mesophyll, this was not consistently observed in the midvein (Fig 3). Freezing in the
388 mesophyll was evident in a 10-20% increase in mean greyscale brightness while freezing in
389 the veins incurred an increase in mean greyscale of <5% (Fig 3). Only one of the eight
390 leaves frozen to -4°C showed a signal of freezing in the midvein, while six of the ten leaves
391 frozen to -5°C showed this signal of freezing.

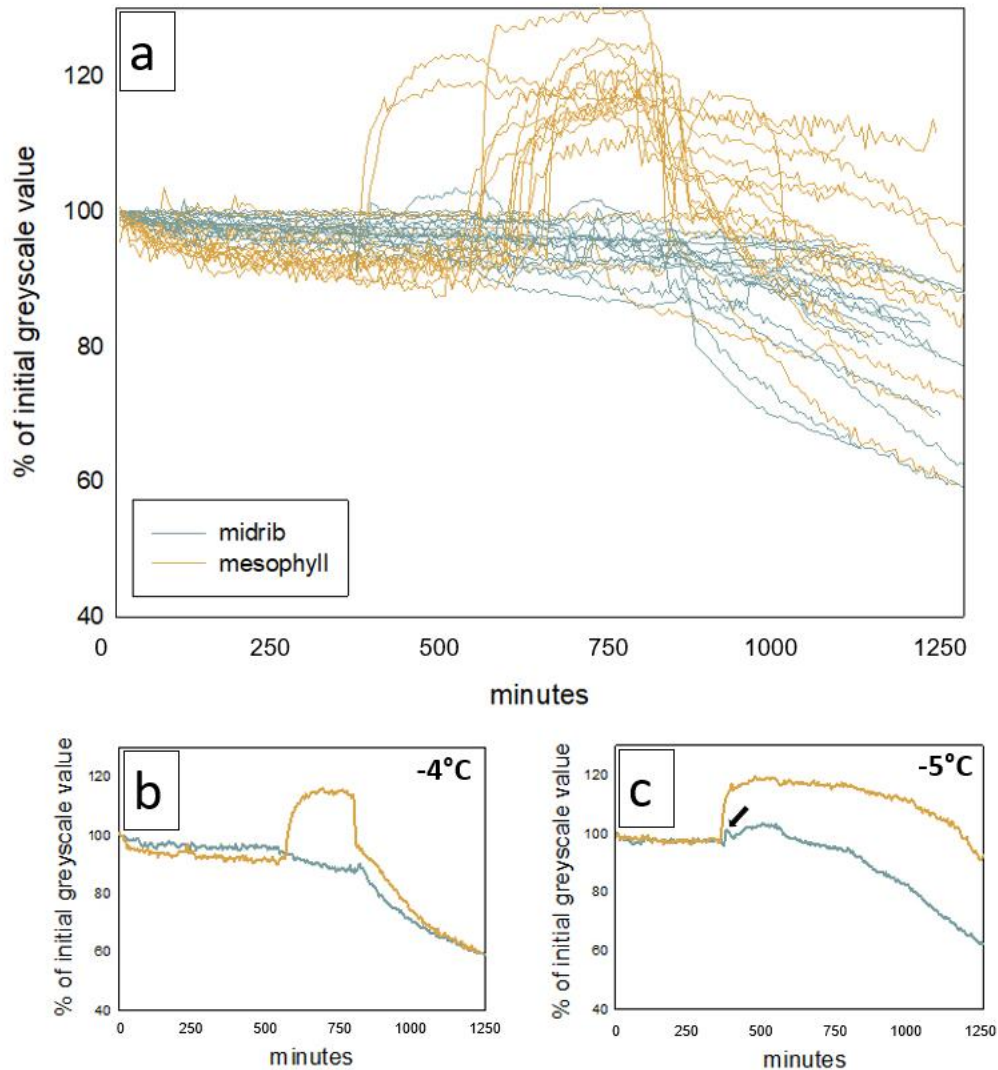
392

393

394

395

396



397

398

399

400

401

402

403

Figure 3: Percentage of initial greyscale value against time for the midvein (midrib) and mesophyll of all *L. tulipifera* leaves frozen to -4°C or -5°C. The mean greyscale values for leaf midveins (blue) and mesophyll adjacent to the midvein (orange) across 250 images (~20 hours) for all leaves frozen to -4°C or -5°C (a). Increases in mean greyscale brightness in the mesophyll (orange) indicate mesophyll freezing. Panel (b) shows the midvein and mesophyll mean greyscale traces for a representative single leaf frozen to -4°C and panel (c) shows the same for a leaf frozen to -5°C with a black arrow denoting the increase in mean greyscale brightness indicating freezing in the midvein.

404

405

406

407

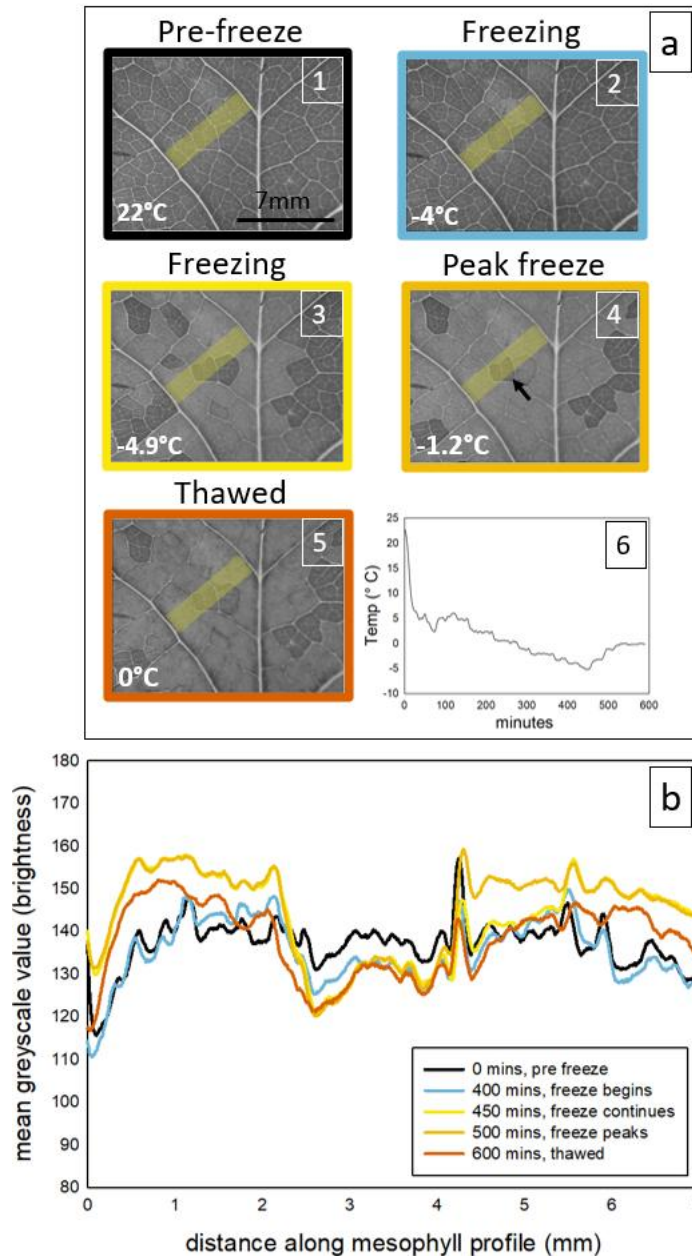
408

409

410

Freezing was first detected in mesophyll immediately adjacent to the midvein and 2° veins, followed by ice propagation away from the vein into areoles bounded by higher order veins (3-5° veins) (Fig. 4). Freezing began at ~ -4°C continuing until 0°C when thawing occurred (Fig. 4). Freezing advanced across the leaf surface in a stepwise pattern between adjacent areoles in discrete patches. Freezing was in some cases not perfectly spatially homogenous, and in all but two leaves where 100% of the area frozen (16 out of 18 leaves) some areoles bounded by third order veins remained unfrozen (Fig. 4, Vid. 1, Fig. S3).

411
412
413
414
415
416
417
418
419
420
421
422
423
424
425
426
427
428
429
430
431



432 **Figure 4:** Representative freezing and thawing sequence including images, mean greyscale value
433 and air temperature for a representative *L. tulipifera* leaf visualised using time-lapse imaging. Panel
434 (a) showed greyscale images of the leaf surface including the midvein and surrounding higher order
435 veins with the transect used to calculates mean greyscale values denotes by a yellow rectangle.
436 Mean greyscale values (b) across a 7mm mean greyscale profile between the midvein and a major
437 vein of *L. tulipifera* leaves measured at 5 stages of freezing in a leaf frozen to -5°C [pre-freeze (1):
438 black, freezing; blue (2) and yellow (3), peak freeze: light orange (4), thawed; terracotta (5)]. The
439 temperature at each stage is in the bottom right-hand corner of each image and panel (6) shows time
440 (minutes) vs temperature (°C). This figure shows the distinctive colour change which occurs with
441 freezing visually (a) and numerically (b), illustrating a situation where a patch in the centre of the

442 mean greyscale profile remains unfrozen (denoted by a black arrow in the 'Peak freeze' image in
443 panel (b)).

444 Freezing at high magnification revealed a similar pattern, where a freezing-front propagated
445 through individual areoles, but then stalled upon reaching a third-order vein boundary (Vid.
446 2). The freezing front can be observed progressing from the bottom left corner towards the
447 middle of the field of view where it can be seen moving through cells before reaching a third-
448 order vein boundary and then progressing to the bottom right and moving towards the middle
449 before reaching the vein boundary in the same manner (Video 1)

450 Thawing, by contrast, did not appear to occur as a staged process, occurring over 1-2
451 images (where images were taken at 5 minutes intervals) when the temperature reached a
452 positive value (0 °C, Fig 4). Thawing resulted in a 'darkening' of the previously lighter frozen
453 patches under the optical cameras which used transmitted light (Fig 2, Fig 4), while thawing
454 corresponded with lightening in the high-resolution video of thawing as this set-up utilised
455 reflected light (Vid. 3). In the hours following thawing, frozen tissue was observed to become
456 red (Fig 5).

457

458

459

460

461

462

463

464

465

466

467

468

469

470

471

472

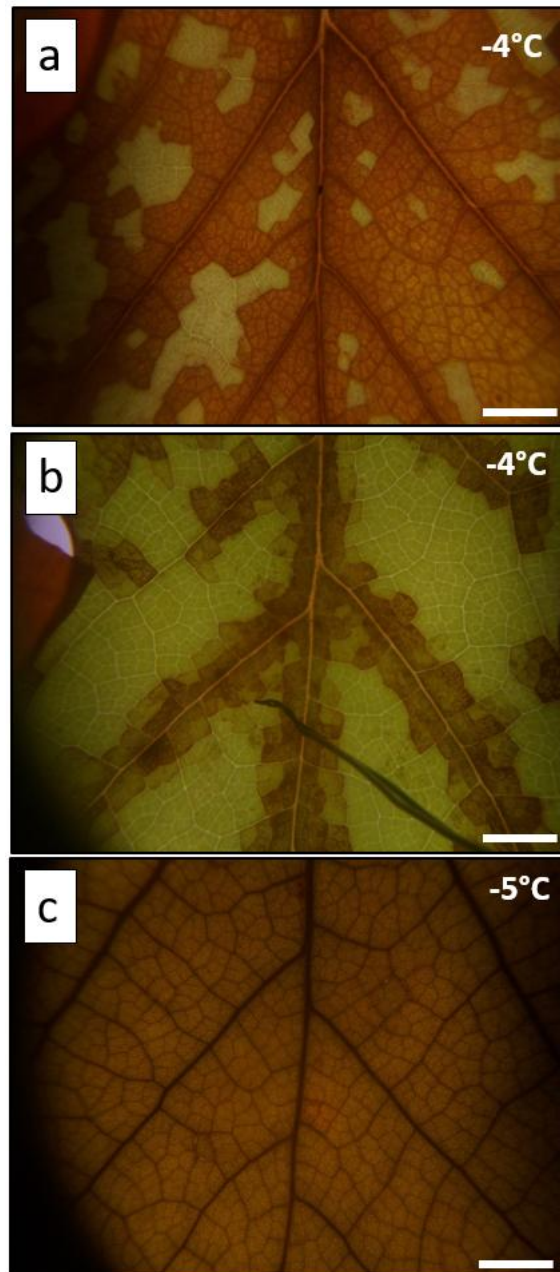
473

474

475

476

477



478

479

480

481

482

Figure 5: *L. tulipifera* leaves ~ 10 hours after thawing, demonstrating the reddening of the tissue that occurred in frozen tissue. This reddening corresponding to the area which was frozen. In leaves frozen to -4° C the patchy-freezing resulted in patchy redness which varied between leaves as demonstrated in (a) and (b), while freezing and therefore reddening affected the entire visible lamina in leaves frozen to -5 ° C (c). Bars = 5mm.

483

Freezing extent

484

485

486

487

Freezing began at an air temperature of -4 °C, with no visible evidence of freezing in leaves exposed to air temperatures of -1°C, -2°C and -3°C. In leaves frozen to -4°C (n = 8), an 58%± 5% of the leaf froze within the camera's field of view, while this increased to 93% ±2% in the ten leaves frozen to -5°C (; P< 0.000008, ANOVA; Fig. 6). Beginning as quickly as 2

488 hours following thawing, veins and frozen mesophyll tissue transitioned to a 'red' colour,
489 further highlighting where freezing had occurred (Fig 5).

490

491

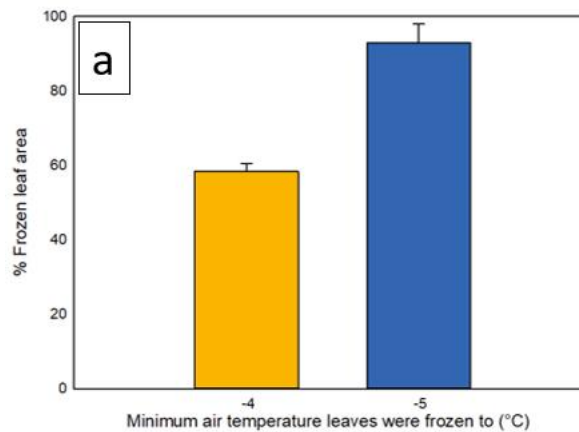
492

493

494

495

496



497

498

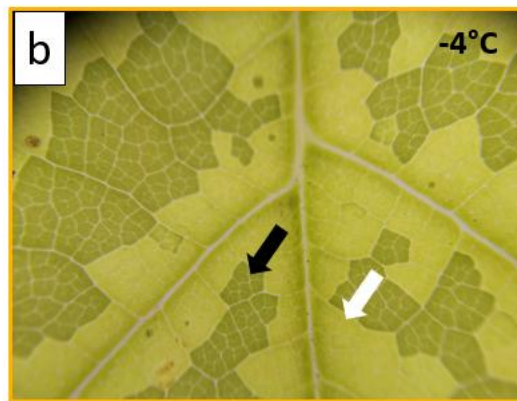
499

500

501

502

503



504

505

506

507

508

509

510



511 **Figure 6:** The percentage frozen leaf area in leaves frozen to air temperatures of -4°C and - 5°C.

512 panel (a) shows to total percentage frozen leaf tissue in all leaves frozen to -4°C (gold) and -5°C

513 (blue). Representative images of the freezing extent are also shown in both a leaf frozen to -4°C (b)

514 and a leaf frozen to -5°C (c). Arrows mark unfrozen tissue (black arrows) and frozen tissue (white

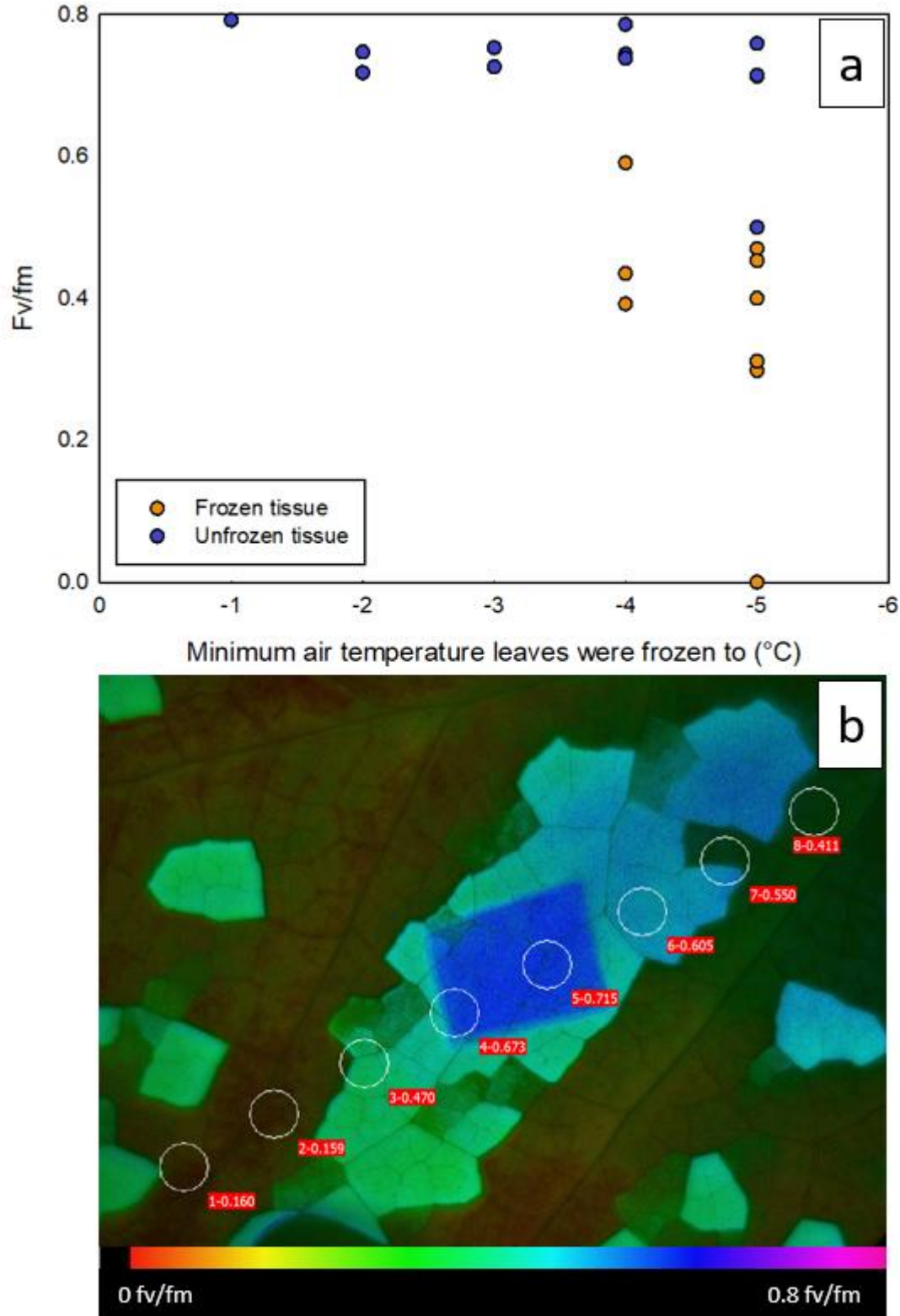
515 arrows) in both (b) and (c).

516 *Chlorophyll Fluorescence Imaging*

517 Chlorophyll fluorescence measured ~6 hours after freezing and thawing invariably

518 decreased in frozen tissue and largely remained high (close to 0.8 Fv/Fm) in tissue which did

519 not freeze (Fig. 7). Mean Fv/Fm for frozen tissue (0.349 ± 0.06) was significantly lower than
520 that for unfrozen tissue (0.733 ± 0.21 ; $P < 0.000003$, ANOVA). In leaves exposed to -1°C -
521 2°C or -3°C , where we observed no freezing of the lamina, fluorescence remained > 0.7
522 Fv/Fm (Fig S four). Evidence of both Fv/Fm depression and high Fv/Fm values in frozen and
523 unfrozen tissue, respectively, were measured in leaves which experienced sub-freezing
524 temperatures (i.e. those exposed to temperatures of -4°C or -5°C). The 'patchy' nature of
525 freezing in the leaf mesophyll visible with the optical camera (Fig.6) was also visible through
526 chlorophyll fluorescence imaging (Figs. 7b, S5).



527

528 **Figure 7:** Changes in chlorophyll fluorescence in response to freezing temperatures in leaves of *L.*
529 *tulipifera*. Panel (a) shows F_v/F_m (photosynthetic capacity) in frozen (orange) and unfrozen (blue)
530 leaf tissue against the minimum air temperature leaves were frozen to, along with a visual
531 representation of fluorescence in a leaf post-freeze (b). The dark blue rectangle in (b) shows the
532 patch of unfrozen tissue which was 'dark-adapted' before the fluorescence measurement, with a value

533 of 0.715 Fv/Fm. Unfrozen tissues outside of this dark-adapted area are turquoise and light green,
534 indicating a higher fluorescence than the surrounding, darker unfrozen tissue. Point values of Fv/fm
535 are shown in eight circular areas of interest arranged diagonally across the image. The colour-scale
536 beneath panel (b) indicates fluorescence values.

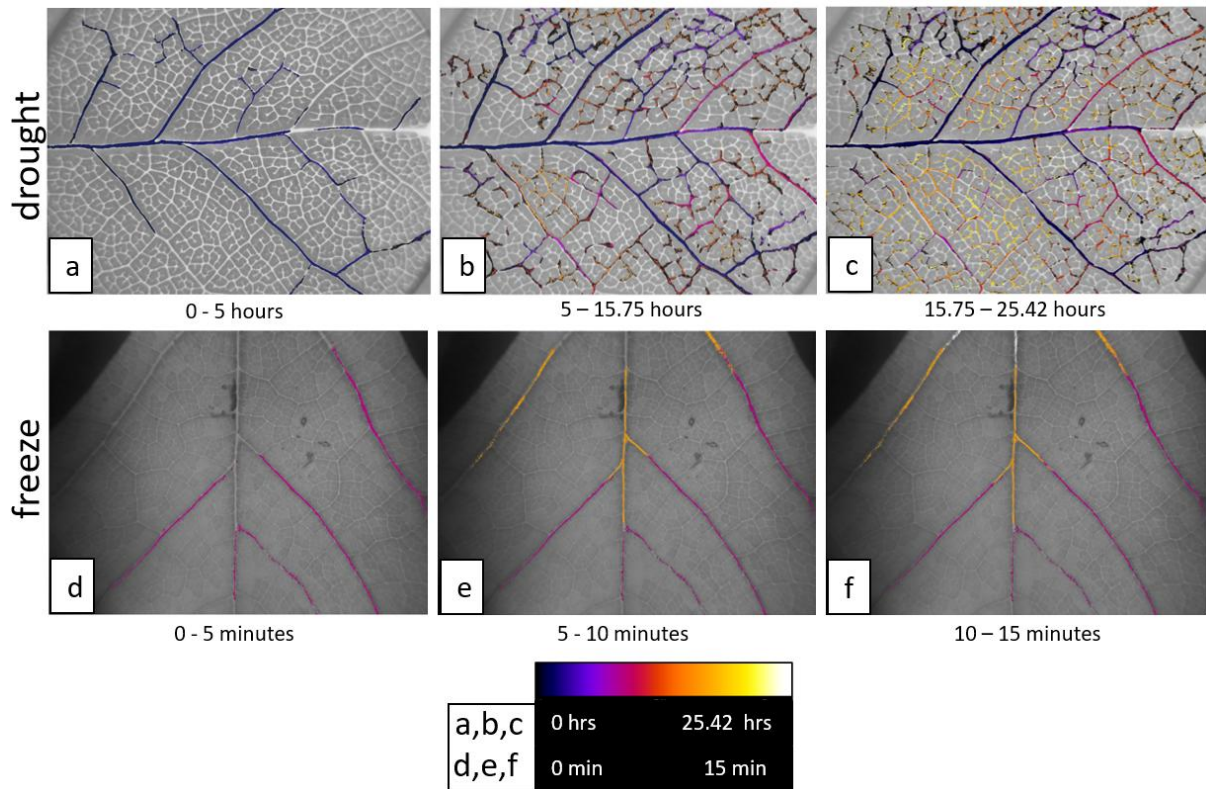
537 *Tree Recovery*

538 While leaves frozen to -4°C or -5°C invariably died, all but one of the 13 trees exposed to
539 these temperatures, which displayed 100% leaf loss, resprouted leaves (Fig. S8). The tree
540 which did not exhibit resprouting was not that which demonstrated the highest percentage of
541 lamina freezing. Resprouting occurred from dormant buds below the leaves frozen during
542 the experiment (Fig. S8)

543 *Freeze-thaw vs. drought-induced embolism*

544 Freeze-thaw embolism was seen in six of the eight leaves frozen to -4°C, but not in any of
545 the leaves frozen to -5°C. Embolism after freezing occurred in 1-3 events and were isolated
546 to the midvein and 2° veins (Fig. S6 Fig.8). We observed no freeze-thaw embolism in the
547 higher order veins, which was distinctly different than the pattern of embolism spread
548 resulting from drought (Fig. 8).

549 Freeze-thaw embolism was confined to the midvein and second order veins, while drought
550 induced embolism was observed in all vein orders (Fig. 8). In leaves where freeze-thaw
551 embolism was observed, 77.6 ± 11.8 % of the midvein and second order veins embolised,
552 compared to 100% of these veins in drought-exposed leaves. In response to drought, the
553 percentage of embolism in tertiary veins and above was a similar to the percentage of
554 freeze-thaw embolised midveins and major veins 74.25 ± 7 %, including all vein orders in
555 drought-exposed leaves (adding major and second order veins) did not alter the percentage
556 of the vein network that was embolised substantially, with $78\% \pm 1.4\%$ of the total vein
557 network found to embolise in leaves exposed to drought. There were far fewer frames which
558 contained embolism in response to freezing and thawing (1-3) than in response to drought
559 (average of 127 ± 24 frames). The midvein and second order veins often embolised first in
560 response to drought embolism (representing $83.56\% \pm 4\%$ of the total embolised area at P₂₅
561 and $76\% \pm 34\%$ of the total embolised length of midveins and second order veins at P₂₅ as a
562 percentage of the total length at P₁₀₀). However, embolism in these veins was accompanied,
563 or shortly followed, by embolism in the minor veins as well (Fig. 8) unlike in leaves exposed
564 to freezing and thawing. The timescale across which drought embolism and freeze thaw-
565 embolised were also very different. While freeze-thaw embolism events occurred within 5-
566 15 minutes, drought induced embolism occurred over a range of 1- 5 days (Fig. 8).



567

568 **Figure 8:** Representative image sequences showing the difference between drought- and freeze-
569 thaw-induced embolism in *L. tulipifera* leaves. Drought-induced embolism spread across 25.42 hours
570 (a, b, c) and freeze-thaw embolism over 15 minutes (d,e,f) in *L. tulipifera* leaves. Panels a, b and c
571 show the progression of drought-induced embolism in four steps of ~23.5 hours each, while the three
572 images in panel (b) show the progression of freeze-thaw embolism in three steps of 5 minutes, where
573 thawing begun at 0 minutes. Embolisms are colour coded according to when they occurred, as
574 indicated by the colour scale beneath each set of images in panels (a) and (b).

575 *Freeze-thaw vs. drought-induced embolism: Stem*

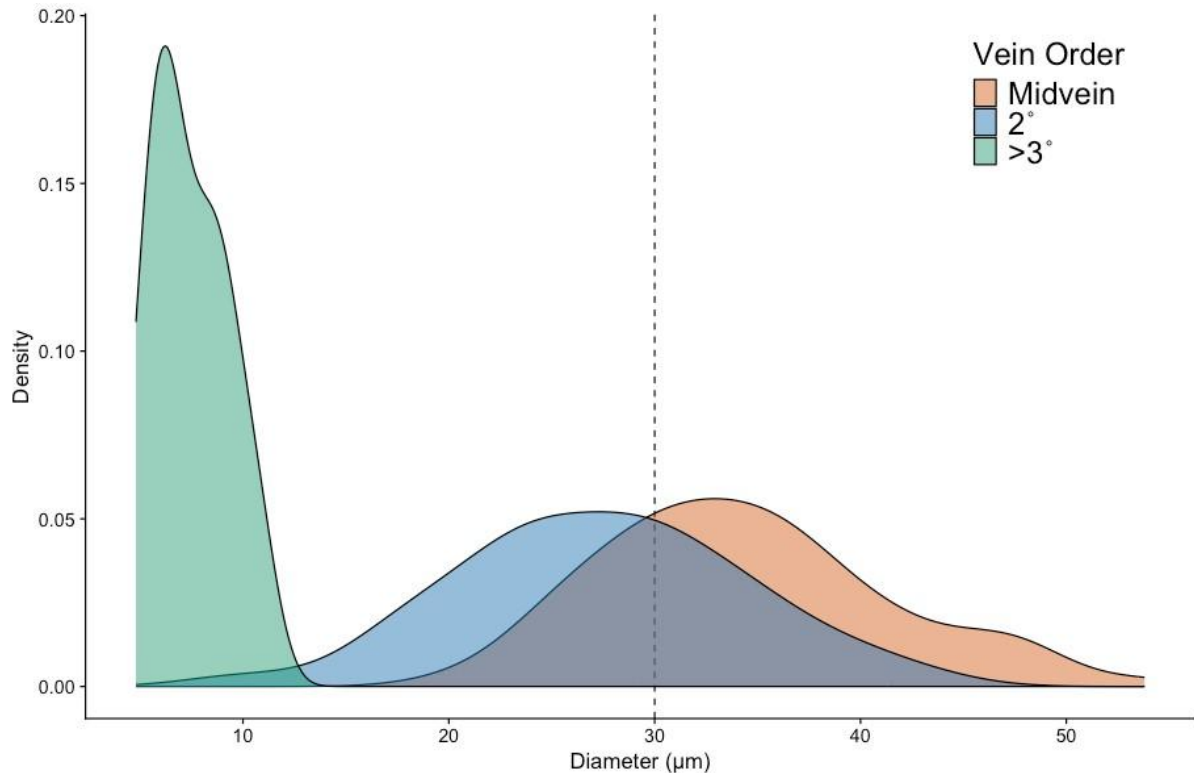
576 A camera placed on the main stem of a tree exposed to a minimum air temperature of -5°C
577 revealed no embolism, though there was evidence of partial freezing in the hydrogel applied
578 to the surface (Fig. S7).

579 *Xylem vessel diameter*

580 We measured vessel lumen diameter distributions in the three lowest vein orders to
581 determine whether this trait might influence vulnerability to freeze-thaw embolism based on
582 the average conduit diameter of 30µm diameter, beyond which a steep increase in freeze-
583 thaw embolism has been observed (Pittermann and Sperry 2003). We found a mean vessel
584 diameter of 34.4 ± 6.96 , 27.4 ± 6.95 , and 7.45 ± 1.85 for the midveins, second order veins,
585 and third order veins, respectively (Fig. 8). We found that 72% and 33.3% of the vessels

586 were greater than 30 μ m in the midveins and second order veins, respectively, but no
587 vessels >30 μ m were found in high order veins.

588



589

590 **Figure 8:** Xylem vessel lumen diameter distributions for leaves of *L. tulipifera*. Distributions are shown
591 for different vein orders (blue = midveins, green = second order veins, orange = high order veins). n =
592 3, mean diameter is statistically different for each group ($p < 0.05$). Vertical dashed line shows the
593 30 μ m threshold, where conduits below this threshold are known to be less vulnerable to freeze-thaw
594 embolism.

595 Discussion

596 Freezing young *L. tulipifera* trees to air temperatures of -4 °C or -5 °C invariably led to visible
597 freezing in the mesophyll, cell damage detected after thawing, and ultimately leaf death. Our
598 visualisations of ice formation in *L. tulipifera* leaves revealed that mesophyll freezing began
599 adjacent to the midveins and second order veins before progressing in a step-wise manner
600 across areoles bounded by third order veins. These freezing patterns support our hypothesis
601 that bundle-sheath extensions (BSEs) strongly influence how ice propagates and spreads
602 through the lamina of these leaves, and possibly all leaves with BSEs. Freeze-thaw
603 embolism occurred only in veins containing vessels with radii 30 μ m or > , in contrast to
604 drought-induced embolism which occurred across all vein orders. This supports our second

605 hypothesis that freeze-thaw embolism is driven by conduit size, agreeing with research in
606 stems, and possibly suggesting that conduit diameter is a major driver of freeze-thaw
607 embolism across all plant organs.

608 *Mesophyll freezing and thawing*

609 Mesophyll freezing, detected with optical cameras, was associated with an increase in pixel
610 brightness, as also recently shown by Kane and McAdam (2024). This increase in brightness
611 can likely be explained by a transition from air to water in the intercellular spaces of the leaf
612 during freezing. This is the same principle that underpins the Optical Vulnerability Technique
613 (OVT) for the observation of drought-induced embolism (Brodribb, Bienaime et al. 2016,
614 Brodribb, Carriqui et al. 2017). The OVT, the original application of the optical cameras used
615 here, detects embolism in leaves as a colour-change from light-coloured translucent xylem
616 (water-filled) to darker air-filled xylem (Brodribb, Carriqui et al. 2017). Therefore, the
617 transition from darker to lighter tissue at freezing temperatures (Kane and McAdam 2024)
618 can likely be explained by the movement of water/ ice into previously air-filled spaces. This
619 idea would also account for the brightening of leaf tissue which remained upon thawing (Fig.
620 4). As the refractive indexes of liquid water (1.33) and ice (1.31) are very similar, the flooded
621 intercellular space would appear brighter even after thawing, as we saw here. This colour
622 change was reversed in the high-resolution freezing, whereby freezing caused a darkening
623 of tissue (Vid. 2). This can be explained by the use of reflected light, rather than transmitted
624 light, further supporting our explanation. The occurrence of intercellular freezing is in-line
625 with the idea of freezing as a dehydration stress in plants (Guy 1990, Steponkus and Webb
626 1992, Ruelland, Vaultier et al. 2009, Vitra, Lenz et al. 2017, Yang, Gerber et al. 2024)
627 whereby water is pulled out of living cells to feed the freezing front in the spaces between
628 cells. In the absence of intracellular freezing, this process is thought to cause tissue death
629 (Steponkus and Webb 1992).

630 The difference in the wave-like spread of freezing from around the midvein and second order
631 veins and the patchy freezing that occurred in mesophyll bound by tertiary veins (Vid 1, Vid
632 2) is likely explained by Bundle-sheath extensions (BSEs). This agrees with research
633 utilising thermal imaging which showed that freezing initiated close to the midvein and
634 second order veins in angiosperm leaves, though freezing could only be tracked up to third
635 order veins in this study (Hacker and Neuner 2007). BSEs have been shown to have
636 numerous functional roles in leaves, including light processing (Barbosa, Chitwood et al.
637 2019), gas exchange (Buckley, Sack et al. 2011) and water relations (Zwieniecki, Brodribb et
638 al. 2007, Kawai, Miyoshi et al. 2017). Our research suggests an additional functional role of
639 these structures, in freezing.

640 Bundle sheath extensions extend to both the upper and lower epidermis in tertiary veins in *L.*
641 *tulipifera* (Fig. S1), but are not present in the midvein or second order veins. BSEs have also
642 been shown to be discontinuous or extend to only one leaf surface in fourth order veins and
643 higher in *L. tulipifera* (Pray 1954). The absence of BSEs in the two lowest vein orders likely
644 accounts for the apparently uninhibited spread of ice adjacent to the midvein and second
645 order veins while their presence may explain the independent and patchy freezing or areoles
646 bounded by tertiary veins (Fig S3). The delay to freezing spread at tertiary vein boundaries
647 in some cases (Vid. 1, Vid. 2), and complete blockage in others is likely explained by BSEs
648 acting as physical barriers to the movement of the ice crystallisation. This suggests that it is
649 not only highly sclerified bundle sheaths like those in *Cinnamomum canphora* that can
650 influence ice propagation (Barbosa, Chitwood et al. 2019).

651 Simultaneous thawing of the leaf tissue also suggests that the physical component of this
652 barrier is more important than chemical differences. If variable solute concentrations in the
653 leaf were governing the pattern of freezing, we might expect thawing of some regions before
654 others. The change to a darker colour upon thawing (Fig. 3), followed by a reddening of
655 affected tissue (Fig. 5) was likely caused by cell lysis (i.e. due to the intrusion of ice crystals)
656 and leakage of electrolytes and other toxic cellular components (Burke, Gusta et al. 1976).
657 Permanent damage to cells after freezing and thawing was clearly evident in the depressed
658 fluorescence (Fig. 7).

659 *Freeze-thaw xylem embolism*

660 Here we present visualisation of freeze-thaw embolism in leaves and evidence of freeze-
661 thaw embolism in real-time, finding that perhaps the most convincing driver of freeze-thaw
662 embolism is conduit size. Freeze-thaw embolism in the lamina was confined to the two
663 lowest vein orders (midvein and second order veins), which also possess the largest vessels
664 (Fig. 8). We found vessel lumen diameters exceeding 30µm in both of the vein orders also
665 showing embolism, with no vessels >15µm in diameter in the third order veins. This aligns
666 with research in conifer stems which shows a sharp increase in vulnerability to freeze-thaw
667 embolism when conduits diameter exceeds 30µm (Pittermann and Sperry 2003) and is
668 consistent with the large body of research in woody plants which shows that larger diameter
669 conduits are at greater risk (Sperry and Sullivan 1992, Sperry, Nichols et al. 1994, Feild and
670 Brodribb 2001, Tyree and Zimmermann 2002, Pittermann and Sperry 2006, Choat, Medek et
671 al. 2011, Robinson, Rennie et al. 2023). This has been theorised (Sevanto, Holbrook et al.
672 2012) and been inferred to be the case in leaves (Ball, Canny et al. 2006) but has, until now,
673 not been visualised in leaves.

674 A reduction in xylem conduit diameter was one of the key adaptations that allowed flowering
675 trees to radiate into freezing environments (Zanne, Tank et al. 2014) and decreasing conduit
676 diameter with increasing probability of freezing temperatures has been observed at a global
677 scale (Sperry 1995, Sevanto, Holbrook et al. 2012). With a large population of vessels
678 <30µm, it is possible that if embolism of the lower vein orders was incomplete, the smaller
679 conduits which are less vulnerable to freeze-thaw embolism could maintain water supply to
680 these leaves. This may allow *L. tulipifera* leaves to resist freeze provided that the
681 photosynthetic tissue are 'hardened' to freezing temperatures. The extent of freezing
682 damage in photosynthetic tissues may, however, outweigh any effects of embolism, at least
683 early in the growing season when leaves are not acclimated for cold temperatures.

684 A mean greyscale signal of freezing in the midvein was observed in six out of the 10 leaves
685 frozen to -5°C but only one out of the 8 frozen to -4°C. This is contrary to evidence from
686 thermal imaging which showed that freezing occurs first in the veins (Hacker and Neuner
687 2007). It is possible that vein freezing is stochastic, occurring base on spontaneous ice
688 nucleation which does not always occur. This may be explained by the nucleation by
689 substances other than water such as macromolecules or dust, termed 'heterogenous
690 nucleation'(Kanji, Ladino et al. 2017, Shardt, Isenrich et al. 2022). Another possibility is that
691 the inconsistency in the detection of freezing in the midvein may be related to the already
692 high transparency of the leaf venation in optical images making the subtle change in the
693 reflective index when water freezes more difficult to detect.

694 A notable factor that we did not test in this study is the speed of freezing and thawing. We
695 opted for a slow freeze-thaw trajectory which mimics field conditions but did not test different
696 speeds of freezing or thawing. Slower freezes are thought to increase the likelihood of
697 freeze-thaw embolism (Sevanto, Holbrook et al. 2012) but slower thawing is thought the
698 decrease the loss of conductivity in the xylem (Langan, Ewers et al. 1997). Given the large
699 increase in percentage frozen area between -4°C and -5°C degrees it's possible that that
700 rapidity of freezing over this one degree temperature range precluded embolism formation
701 and that a slower freeze or thaw may have produced different results.

702 *Freeze-thaw vs. drought induced xylem embolism*

703 Differences in the mechanism behind embolism induced by drought vs. freeze-thaw
704 embolism in the leaf lamina likely explains the contrasting extent of embolism observed in *L.*
705 *tulipifera* leaves exposed to freezing and drought. Importantly, the clear visibility of embolism
706 in higher order veins in leaves exposed to drought means that we can be sure that the lack
707 of embolism in their higher order veins in frozen leaves was not a failure of the optical
708 cameras to detect these events, but an absence of embolism in these vein orders. The

709 vulnerability of xylem conduits to air-seeding under drought conditions has been linked
710 anatomical characteristics such as the thickness of the pit membranes in the xylem wall (the
711 site at which air enters, causing embolism due to drought;Thonglim, Delzon et al. 2021,
712 Thonglim, Bortolami et al. 2023) and connectivity of the xylem network (Brodersen and
713 Roddy 2016, Johnson, Brodersen et al. 2020, Mrad, Johnson et al. 2020). Combined, these
714 anatomical features likely explain the pattern of drought-induced embolism we observed in
715 young *L. tulipifera* leaves whereby embolism progressed through the major vein orders
716 terminating in the higher order veins, a pattern which is consistently observed across the
717 leaves of woody and herbaceous angiosperms (Johnson, Jordan et al. 2018, Tonet, Carins-
718 Murphy et al. 2023). In contrast, freeze-thaw embolism in the lamina, likely caused by gas
719 segregation and subsequent bubble expansion (Sevanto, Holbrook et al. 2012), is thought to
720 be determined primarily by xylem diameter (Pittermann and Sperry 2006). This, as described
721 above, may explain why freeze-thaw embolism occurred only in the largest veins in *L.*
722 *tulipifera*, where we found that 72% and 33.3% of the vessels in the midveins and second
723 order veins, respectively, were above the 30 μ m threshold. Conduit size is shown to be a
724 poor predictor of drought-induced xylem embolism resistance (Lens, Gleason et al. 2022)
725 and connectivity and xylem-pit-properties unlikely to have any influence on the formation of
726 freeze-thaw embolism. It is therefore likely that differences in the drivers of drought and
727 freeze-thaw embolism cause the differences we observed in the extent of embolism in *L.*
728 *tulipifera* leaf venation networks. This evidence strongly supports that idea that conduit
729 diameter plays a mechanistic role in freeze-thaw embolism.

730 *What kills L. tulipifera leaves during a freeze? Freezing as a drought stress*

731 The freeze-induced embolism and damage to living cells detected here highlights that
732 freezing can affect both the water transport and photosynthetic systems in young *L. tulipifera*
733 leaves. It should also be noted however, that regardless of whether embolism occurred, all
734 leaves which showed evidence of mesophyll freezing subsequently died. Cell damage and
735 death was evident in all leaves that froze. All leaves in trees exposed to temperatures below
736 -4°C died after thawing, clearly evident in leaf browning within days of freezing and thawing
737 (Fig. S8). This lethal damage was also evident in the notable depression of fluorescence in
738 frozen mesophyll (Fig. 7), and the 'red' appearance of the leaves in the hours following
739 thawing indicating cell-rupture (Fig.5). Additionally, *L. tulipifera* leaves presented 'wilted and
740 wet' after thawing, a state described by Burke and Gusta et al (1976) in observations of
741 young spring leaves after frost events, attributed to the loss of semi permeability in the cell
742 membranes. Importantly, a lack of fluorescence decline in leaves where freezing was not
743 observed, (those frozen to -1°C, -2°C and -3°C) indicates that fluorescence values were not
744 impacted by the time spent in the freezer or the placement of cameras on leaves (Fig. S4).

745 The absence of embolism in the lamina of leaves frozen to -5°C indicates that embolism in
746 the lamina is not necessary to induce leaf-death.

747 *The fate of L. tulipifera leaves exposed to freeze*

748 The wide-vesseled, soft, broad leaves of winter-deciduous *L. tulipifera* trees are clearly not
749 adapted to survive freezing in spring. Our results suggest that onset of freezing damage
750 represents the point of no-return in these leaves, with freezing found to progress over a
751 narrow air-temperature range expanding from 60% to nearly 100% of the leaf area frozen
752 across just 1°C . While the death of living cells was ultimately the cause of mortality in these
753 leaves, the water transport system is inherently compromised because of freezing. With
754 xylem conduit size fixed at the time of leaf development, the large diameter vessels of the
755 midvein and second order veins in the leaf lamina likely make *L. tulipifera* leaves susceptible
756 to freeze thaw embolism throughout the growing season. However, high redundancy of
757 conduits in the two lowest vein orders, and a large proportion of vessels below the $30\mu\text{m}$
758 threshold, may allow leaves to continue to function provided that the mesophyll and other
759 tissues is frost-hardened (Vitra, Lenz et al. 2017).

760 **Conclusions**

761 Freezing invariably killed *L. tulipifera* leaves. Death of living tissue was a constant,
762 sometimes accompanied by freeze-thaw embolism which occurred rapidly and was confined
763 to the veins with the largest conduits, in stark contrast to drought-induced embolism. This
764 supports research in stems showing that conduit diameter drives freeze-thaw embolism
765 vulnerability. The progression of freezing through the mesophyll in patches bounded by
766 tertiary veins implicates BSEs in driving lateral ice propagation. While freezing in the
767 mesophyll conclusively led to death in *L. tulipifera* leaves, a significant proportion of xylem
768 vessels were inherently vulnerable to freeze-thaw embolism, showing that spring frost
769 results in a dual mode of lethality in *L. tulipifera* leaves.

770 **Acknowledgements**

771 KMJ was supported by a Fulbright Future Postdoctoral Fellowship Awarded by the
772 Australian Fulbright Foundation and the Kinghorn Foundation. RWS, MS and DG were
773 supported by Swiss National Science Foundation grant: 200021-212066.

774 **Author contributions**

775 KMJ and CRB conceived and designed the study. KMJ and CRB conducted experiments
776 and measurements using optical cameras and microscopy, while KMJ and MS designed and
777 conducted the collection of high-resolution imagery with guidance from DG, RWS and ERD.
778 KMJ and CRB wrote the manuscript with contributions from all authors.

779 **Competing Interests**

780 None declared

781 **Data availability**

782 The data will be made available by the corresponding authors upon reasonable request.

783 **Supporting Information**

784 **Figure S1:** Transverse light microscope section of the lamina of a *Liriodendron tulipifera* leaf
785 highlighting a bundle-sheath extension.

786 **Figure S2:** Comparison of natural and experimental freezing trajectories.

787 **Video 1:** The pattern of freezing and thawing detected in a leaf frozen to -5 ° C with time-lapse
788 imaging.

789 **Figure S3:** Examples of the 'patchy' nature of freezing observed in *Liriodendron tulipifera* leaves
790 frozen to air temperatures of both -4 ° C and -5 ° C.

791 **Figure S4:** Chlorophyll fluorescence (Fv/Fm) in *Liriodendron tulipifera* leaves which were placed in
792 the freezer but did not show visible signs of freezing.

793 **Figure S5:** Comparison of optically resolved freezing and cell damage shown through imaging
794 fluorescence in *Liriodendron tulipifera* leaves.

795 **Figure S6:** The total embolism overlaid onto initial images of each the six *Liriodendron tulipifera*
796 leaves in which embolism was observed.

797 **Figure S7:** The changes to the tensile hydrogel applied to the surface of the stem of a *Liriodendron*
798 *tulipifera* tree during freezing.

799 **Video 2:** High resolution freezing in a *Liriodendron tulipifera* leaf.

800 **Video 3:** High resolution GIF of thawing of a *Liriodendron tulipifera* leaf.

801 **Figure S8:** *Liriodendron tulipifera* trees shortly after they were exposed to -4°C or -5°C freeze
802 treatments.

803 References

- 804 (2016). R: A language and environment for statistical computing. R Foundation for Statistical
805 Computing Vienna, Austria R Core Team.
- 806 Ashworth, E. N. and R. S. Pearce (2002). "Extracellular freezing in leaves of freezing-sensitive
807 species." *Planta* **214**(5): 798-805.
- 808 Ball, M. C., M. J. Canny, C. X. Huang, J. J. G. Egerton and J. Wolfe (2006). "Freeze/thaw-induced
809 embolism depends on nadir temperature: the heterogeneous hydration hypothesis." *Plant, Cell &*
810 *Environment* **29**(5): 729-745.
- 811 Barbosa, M. A. M., D. H. Chitwood, A. A. Azevedo, W. L. Araújo, D. M. Ribeiro, L. E. P. Peres, S. C. V.
812 Martins and A. Zsögön (2019). "Bundle sheath extensions affect leaf structural and physiological
813 plasticity in response to irradiance." *Plant, Cell & Environment* **42**(5): 1575-1589.
- 814 Brodersen, C. R. and A. B. Roddy (2016). "New frontiers in the three-dimensional visualization of
815 plant structure and function." *Am J Bot* **103**(2): 184-188.
- 816 Brodrribb, T., C. R. Brodersen, M. Carriqui, V. Tonet, C. Rodriguez Dominguez and S. McAdam (2021).
817 "Linking xylem network failure with leaf tissue death." *New Phytologist* **n/a**(n/a).
- 818 Brodrribb, T. J., D. Bienaime and P. Marmottant (2016). "Revealing catastrophic failure of leaf
819 networks under stress." *PNAS* **113**(17): 4865-4869.
- 820 Brodrribb, T. J., M. Carriqui, S. Delzon and C. Lucani (2017). "Optical Measurement of Stem Xylem
821 Vulnerability." *Plant Physiol* **174**(4): 2054-2061.
- 822 Buckley, T. N., L. Sack and M. E. Gilbert (2011). "The Role of Bundle Sheath Extensions and Life Form
823 in Stomatal Responses to Leaf Water Status." *Plant Physiology* **156**(2): 962-973.
- 824 Burke, M., L. Gusta, H. Quamme, C. Weiser and P. Li (1976). "Freezing and injury in plants." *Annual*
825 *Review of Plant Physiology* **27**(1): 507-528.
- 826 Cavender-Bares, J., P. Cortes, S. Rambal, R. Joffre, B. Miles and A. Rocheteau (2005). "Summer and
827 winter sensitivity of leaves and xylem to minimum freezing temperatures: a comparison of co-
828 occurring Mediterranean oaks that differ in leaf lifespan." *New Phytologist* **168**(3): 597-612.
- 829 Choat, B., D. E. Medek, S. A. Stuart, J. Pasquet-Kok, J. J. G. Egerton, H. Salari, L. Sack and M. C. Ball
830 (2011). "Xylem traits mediate a trade-off between resistance to freeze-thaw-induced embolism and
831 photosynthetic capacity in overwintering evergreens." *New Phytologist* **191**(4): 996-1005.
- 832 Cobb, A. R., B. Choat and N. M. Holbrook (2007). "Dynamics of freeze-thaw embolism in *Smilax*
833 *rotundifolia* (Smilacaceae)." *American Journal of Botany* **94**(4): 640-649.
- 834 Davis, S. D., J. S. Sperry and U. G. Hacke (1999). "The relationship between xylem conduit diameter
835 and cavitation caused by freezing." *American Journal of Botany* **86**(10): 1367-1372.
- 836 Esau, K. (1960). "Anatomy of Seed Plants." *Soil Science* **90**(2): 149.
- 837 Ewers, F. W. (1985). "Xylem' Structure and Water Conduction in Conifer Trees, Dicot Trees, and
838 Llanas." *IAWA Journal* **6**(4): 309-317.
- 839 Feild, T. S. and T. Brodrribb (2001). "Stem water transport and freeze-thaw xylem embolism in
840 conifers and angiosperms in a Tasmanian treeline heath." *Oecologia* **127**(3): 314-320.
- 841 Gerber, D., L. A. Wilen, E. R. Dufresne and R. W. Style (2023). "Polycrystallinity Enhances Stress
842 Buildup around Ice." *Physical Review Letters* **131**(20): 208201.
- 843 Gusta, L. V., M. Wisniewski, N. T. Nesbitt and M. L. Gusta (2004). "The effect of water, sugars, and
844 proteins on the pattern of ice nucleation and propagation in acclimated and nonacclimated canola
845 leaves." *Plant Physiol* **135**(3): 1642-1653.
- 846 Guy, C. L. (1990). "Cold acclimation and freezing stress tolerance: role of protein metabolism."
847 *Annual review of plant biology* **41**(1): 187-223.
- 848 Hacke, U. and J. Sauter (1996). "Xylem dysfunction during winter and recovery of hydraulic
849 conductivity in diffuse-porous and ring-porous trees." *Oecologia* **105**: 435-439.
- 850 Hacker, J. and G. Neuner (2007). "Ice propagation in plants visualized at the tissue level by infrared
851 differential thermal analysis (IDTA)." *Tree Physiology* **27**(12): 1661-1670.
- 852 Hammel, H. T. (1967). "Freezing of Xylem Sap without Cavitation." *Plant Physiology* **42**(1): 55-66.

- 853 Johnson, K. M., C. R. Brodersen, M. R. Carins-Murphy, B. Choat and T. J. Brodribb (2020). "Xylem
854 embolism spreads by single-conduit events in three dry forest angiosperm stems." Plant Physiology
855 **184**: 212-222.
- 856 Johnson, K. M., G. J. Jordan and T. J. Brodribb (2018). "Wheat leaves embolized by water stress do
857 not recover function upon rewatering." Plant Cell Environ **41**(11): 2704-2714.
- 858 Kane, C. N. and S. A. M. McAdam (2024). "Spatial and Temporal Freezing Dynamics of Leaves
859 Revealed by Time-Lapse Imaging." Plant, Cell & Environment **n/a**(n/a).
- 860 Kanji, Z. A., L. A. Ladino, H. Wex, Y. Boose, M. Burkert-Kohn, D. J. Cziczo and M. Krämer (2017).
861 "Overview of Ice Nucleating Particles." Meteorological Monographs **58**: 1.1-1.33.
- 862 Karabourniotis, G., J. F. Bornman and D. Nikolopoulos (2000). "A possible optical role of the bundle
863 sheath extensions of the heterobaric leaves of *Vitis vinifera* and *Quercus coccifera*." Plant, Cell &
864 Environment **23**(4): 423-430.
- 865 Kawai, K., R. Miyoshi and N. Okada (2017). "Bundle sheath extensions are linked to water relations
866 but not to mechanical and structural properties of leaves." Trees **31**: 1227-1237.
- 867 Kokin, E., M. Pennar, V. Palge and K. Jürjenson (2018). "Strawberry leaf surface temperature
868 dynamics measured by thermal camera in night frost conditions."
- 869 Lang, G. A. (1987). "Dormancy: a new universal terminology."
- 870 Langan, S. J., F. W. Ewers and S. D. Davis (1997). "Xylem dysfunction caused by water stress and
871 freezing in two species of co-occurring chaparral shrubs." Plant, Cell & Environment **20**(4): 425-437.
- 872 Larcher, W., U. Meindl, E. Ralsler and M. Ishikawa (1991). "Persistent Supercooling and Silica
873 Deposition in Cell Walls of Palm Leaves." Journal of Plant Physiology **139**(2): 146-154.
- 874 Lens, F., S. M. Gleason, G. Bortolami, C. Brodersen, S. Delzon and S. Jansen (2022). "Functional xylem
875 characteristics associated with drought-induced embolism in angiosperms." New Phytologist **236**(6):
876 2019-2036.
- 877 Li, Z., D. Luo, M. M. Ibrahim, E. Hou and C. Wang (2024). "Adaptive strategies to freeze-thaw cycles
878 in branch hydraulics of tree species coexisting in a temperate forest." Plant Physiology and
879 Biochemistry **206**: 108223.
- 880 Loehle, C. (1998). "Height growth rate tradeoffs determine northern and southern range limits for
881 trees." Journal of Biogeography **25**(4): 735-742.
- 882 Lütz, C. (2010). "Cell physiology of plants growing in cold environments." Protoplasma **244**(1): 53-73.
- 883 Mayr, S., P. Schmid, J. Laur, S. Rosner, K. Charra-Vaskou, B. Dämon and U. G. Hacke (2014). "Uptake
884 of Water via Branches Helps Timberline Conifers Refill Embolized Xylem in Late Winter " Plant
885 Physiology **164**(4): 1731-1740.
- 886 Mazur, P. (1969). "Freezing Injury in Plants." Annual Review of Plant Biology **20**(Volume 20, 1969):
887 419-448.
- 888 Mrad, A., D. M. Johnson, D. M. Love and J.-C. Domec (2020). "The roles of conduit redundancy and
889 connectivity in xylem hydraulic functions." New Phytol.
- 890 Muffler, L., C. Beierkuhnlein, G. Aas, A. Jentsch, A. H. Schweiger, C. Zohner and J. Kreyling (2016).
891 "Distribution ranges and spring phenology explain late frost sensitivity in 170 woody plants from the
892 Northern Hemisphere." Global Ecology and Biogeography **25**(9): 1061-1071.
- 893 Neger, F. W. (1918). "Die Wegsamkeit der Laubblätter für Gase." Flora oder Allgemeine Botanische
894 Zeitung **111**: 152-161.
- 895 Nilsson, O. (2022). "Winter dormancy in trees." Current Biology **32**(12): R630-R634.
- 896 Pieruschka, R., U. Schurr, M. Jensen, W. F. Wolff and S. Jahnke (2006). "Lateral diffusion of CO₂ from
897 shaded to illuminated leaf parts affects photosynthesis inside homobaric leaves." New Phytologist
898 **169**(4): 779-788.
- 899 Pittermann, J. and J. Sperry (2003). "Tracheid diameter is the key trait determining the extent of
900 freezing-induced embolism in conifers." Tree Physiology **23**(13): 907-914.
- 901 Pittermann, J. and J. S. Sperry (2006). "Analysis of Freeze-Thaw Embolism in Conifers. The Interaction
902 between Cavitation Pressure and Tracheid Size." Plant Physiology **140**(1): 374-382.

- 903 Pray, T. R. (1954). "Foliar Venation of Angiosperms. I. Mature Venation of Liriodendron." American
904 Journal of Botany **41**(8): 663-670.
- 905 Robinson, J. A., M. Rennie, M. Clearwater, D. J. Holland, A. K. van den Berg and M. Watson (2023).
906 "Examination of embolisms in maple and birch saplings utilising microCT." Micron **168**: 103438.
- 907 Ruelland, E., M.-N. Vaultier, A. Zachowski and V. Hurry (2009). Chapter 2 Cold Signalling and Cold
908 Acclimation in Plants. Advances in Botanical Research, Academic Press. **49**: 35-150.
- 909 Sakai, A. and W. Larcher (2012). Frost survival of plants: responses and adaptation to freezing stress,
910 Springer Science & Business Media.
- 911 Sapkota, S., M. Salem, K. R. Jahed, T. S. Artlip and S. M. Sherif (2023). "From endodormancy to
912 ecodormancy: the transcriptional landscape of apple floral buds." Front Plant Sci **14**: 1194244.
- 913 Schindelin, J., I. Arganda-Carreras, E. Frise, V. Kaynig, M. Longair, T. Pietzsch, S. Preibisch, C. Rueden,
914 S. Saalfeld, B. Schmid, J.-Y. Tinevez, D. J. White, V. Hartenstein, K. Eliceiri, P. Tomancak and A.
915 Cardona (2012). "Fiji: an open-source platform for biological-image analysis." Nature Methods **9**(7):
916 676-682.
- 917 Sevanto, S., N. M. Holbrook and M. Ball (2012). "Freeze/Thaw-Induced Embolism: Probability of
918 Critical Bubble Formation Depends on Speed of Ice Formation." Frontiers in Plant Science **3**.
- 919 Shardt, N., F. N. Isenrich, B. Waser, C. Marcolli, Z. A. Kanji, A. J. deMello and U. Lohmann (2022).
920 "Homogeneous freezing of water droplets for different volumes and cooling rates." Physical
921 Chemistry Chemical Physics **24**(46): 28213-28221.
- 922 Sperry, J. S. (1995). 5 - Limitations on Stem Water Transport and Their Consequences. Plant Stems. B.
923 L. Gartner. San Diego, Academic Press: 105-124.
- 924 Sperry, J. S., J. R. Donnelly and M. T. Tyree (1988). "SEASONAL OCCURRENCE OF XYLEM EMBOLISM
925 IN SUGAR MAPLE (ACER SACCHARUM)." American Journal of Botany **75**(8): 1212-1218.
- 926 Sperry, J. S., K. L. Nichols, J. E. M. Sullivan and S. E. Eastlack (1994). "Xylem Embolism in Ring-Porous,
927 Diffuse-Porous, and Coniferous Trees of Northern Utah and Interior Alaska." Ecology **75**(6): 1736-
928 1752.
- 929 Sperry, J. S. and J. E. M. Sullivan (1992). "Xylem Embolism in Response to Freeze-Thaw Cycles and
930 Water Stress in Ring-Porous, Diffuse-Porous, and Conifer Species 1." Plant Physiology **100**(2): 605-
931 613.
- 932 Stegner, M., O. Buchner, M. Geßlbauer, J. Lindner, A. Flörl, N. Xiao, A. Holzinger, N. Gierlinger and G.
933 Neuner (2023). "Frozen mountain pine needles: The endodermis discriminates between the ice-
934 containing central tissue and the ice-free fully functional mesophyll." Physiologia Plantarum **175**(1):
935 e13865.
- 936 Steponkus, P. and M. Webb (1992). Freeze-induced dehydration and membrane destabilization in
937 plants. Water and Life: Comparative Analysis of Water Relationships at the Organismic, Cellular, and
938 Molecular Levels, Springer: 338-362.
- 939 Steponkus, P. L., M. F. Dowgert and W. J. Gordon-Kamm (1983). "Destabilization of the plasma
940 membrane of isolated plant protoplasts during a freeze-thaw cycle: The influence of cold
941 acclimation." Cryobiology **20**(4): 448-465.
- 942 Thonglim, A., G. Bortolami, S. Delzon, M. Larter, R. Offringa, J. J. B. Keurentjes, E. Smets, S. Balazadeh
943 and F. Lens (2023). "Drought response in Arabidopsis displays synergistic coordination between
944 stems and leaves." Journal of Experimental Botany **74**(3): 1004-1021.
- 945 Thonglim, A., S. Delzon, M. Larter, O. Karami, A. Rahimi, R. Offringa, J. J. B. Keurentjes, S. Balazadeh,
946 E. Smets and F. Lens (2021). "Intervessel pit membrane thickness best explains variation in embolism
947 resistance amongst stems of Arabidopsis thaliana accessions." Annals of Botany **128**(2): 171-182.
- 948 Tonet, V., M. Carins-Murphy, R. Deans and T. J. Brodribb (2023). "Deadly acceleration in dehydration
949 of Eucalyptus viminalis leaves coincides with high-order vein cavitation." Plant Physiology **191**(3):
950 1648-1661.
- 951 Trifiló, P., F. Raimondo, T. Savi, M. A. Lo Gullo and A. Nardini (2016). "The contribution of vascular
952 and extra-vascular water pathways to drought-induced decline of leaf hydraulic conductance."
953 Journal of Experimental Botany **67**(17): 5029-5039.

954 Tyree, M. T. and M. H. Zimmermann (2002). Xylem structure and the ascent of sap, Springer Science
955 & Business Media.

956 Vitasse, Y., A. Bottero, M. Cailleret, C. Bigler, P. Fonti, A. Gessler, M. Lévesque, B. Rohner, P. Weber,
957 A. Rigling and T. Wohlgemuth (2019). "Contrasting resistance and resilience to extreme drought and
958 late spring frost in five major European tree species." Global Change Biology **25**(11): 3781-3792.

959 Vitra, A., A. Lenz and Y. Vitasse (2017). "Frost hardening and dehardening potential in temperate
960 trees from winter to budburst." New Phytologist **216**(1): 113-123.

961 Wise, R. R. (1995). "Chilling-enhanced photooxidation: The production, action and study of reactive
962 oxygen species produced during chilling in the light." Photosynthesis Research **45**(2): 79-97.

963 Wisniewski, M. and M. Fuller (1999). Ice nucleation and deep supercooling in plants: new insights
964 using infrared thermography. Cold-Adapted Organisms: Ecology, Physiology, Enzymology and
965 Molecular Biology. R. Margesin and F. Schinner. Berlin, Heidelberg, Springer Berlin Heidelberg: 105-
966 118.

967 Wylie, R. B. (1943). "The Role of the Epidermis in Foliar Organization and its Relations to the Minor
968 Venation." American Journal of Botany **30**(4): 273-280.

969 Wylie, R. B. (1952). "The Bundle Sheath Extension in Leaves of Dicotyledons." American Journal of
970 Botany **39**(9): 645-651.

971 Yang, S., D. Gerber, Y. Feng, N. Bain, M. Kuster, L. de Lorenzis, Y. Xu, E. R. Dufresne and R. W. Style
972 (2024). "Dehydration drives damage in the freezing of brittle hydrogels." arXiv preprint
973 arXiv:2401.12871.

974 Yarberry, W. and W. Yarberry (2021). "Dplyr." CRAN recipes: DPLYR, stringr, lubridate, and regex in
975 R: 1-58.

976 Zanne, A. E., D. C. Tank, W. K. Cornwell, J. M. Eastman, S. A. Smith, R. G. FitzJohn, D. J. McGlenn, B. C.
977 O'Meara, A. T. Moles, P. B. Reich, D. L. Royer, D. E. Soltis, P. F. Stevens, M. Westoby, I. J. Wright, L.
978 Aarssen, R. I. Bertin, A. Calaminus, R. Govaerts, F. Hemmings, M. R. Leishman, J. Oleksyn, P. S. Soltis,
979 N. G. Swenson, L. Warman and J. M. Beaulieu (2014). "Three keys to the radiation of angiosperms
980 into freezing environments." Nature **506**(7486): 89-92.

981 Zhang, P., B. Han, P. Ding and J.-J. Zhu (2023). "An approach to quantify the free water content in
982 leaves of *Quercus acutissima* Carruth. with differential thermal analysis." Plant Science
983 Journal **41**(5): 687-693.

984 Zwieniecki, M. A., T. J. Brodribb and N. M. Holbrook (2007). "Hydraulic design of leaves: insights from
985 rehydration kinetics." Plant, Cell & Environment **30**(8): 910-921.

986